N-Acylphosphatidylethanolamines: Effect of the *N*-Acyl Chain Length on Its Orientation

Claude-Paul Lafrance, Jean-Érik Blochet, and Michel Pézolet
Centre de Recherches en Sciences et Ingénierie des Macromolécules and Département de Chimie, Université Laval, Québec G1K 7P4, Canada

ABSTRACT *N*-Acylphosphatidylethanolamines, or NAPEs, are found in tissues involved in degenerating processes, such as dehydrated endosperm of seeds, erythrocyte membranes, or cell injury. To determine the conformation and orientation of the acyl chains of these phospholipids, NAPEs with deuterated *N*-acyl chains of 6 and 16 carbon atoms were synthesized and studied by transmission and attenuated total reflectance (ATR) infrared spectroscopy. For *N*-C16d-DPPE, the ATR measurements show that the *N*-acyl chain has the same orientation as the two acyl chains attached to the glycerol moiety, while the *N*-acyl chain of *N*-C6d-DPPE is randomly oriented. These results demonstrate that for *N*-C16d-DPPE, the *N*-acyl chain is embedded into the hydrophobic core of the bilayer, while for the short chain derivative the *N*-acyl chain remains in the lipid headgroup region. The analysis of the carbonyl stretching band and of the amide I band suggests that, for the long *N*-acyl chain lipid, the ester C═O and the N–H groups are linked by intermolecular hydrogen bonds.

INTRODUCTION

N-Acyl derivatives of phosphatidylethanolamines (PE) are membrane components that were first isolated from the wheat endosperm (Bomstein, 1965), where they account for ~50% of the polar lipids. Later, they have been found in various microorganisms, plants, and animal tissues (see Chapman and Moore, 1993). These lipids, which originate from the acylation of zwitterionic phospholipids, usually accumulate in cells during degenerative processes such as desiccation in plant seeds or myocardial infarct in animals.

The structure of aqueous dispersions of NAPE with a saturated *N*-acyl chain is mainly lamellar, whether the acyl chains attached to the glycerol moiety are saturated or unsaturated (Newman et al., 1986; Akoka et al., 1988). Studies of the thermotropic behavior of synthetic NAPEs by differential scanning calorimetry and ^{31}P nuclear magnetic resonance spectroscopy (NMR) have shown that the temperature of the gel-to-liquid crystalline (LC) phase transition depends on the *N*-acyl chain length, which also affects the polar headgroup mobility (Akoka et al., 1988). In the gel phase, *N*-caproyl-PE displays a rapid axial rotation, whereas derivatives with longer *N*-acyl chains display a highly restricted headgroup motion. More recently, Lafrance et al. (1990) have followed by Raman and infrared spectroscopy the acyl chain conformation and the polar headgroup hydration as a function of the sample temperature. They have shown that *N*-acyl derivatives of dipalmitoylphosphatidylethanolamine (DPPE) can be divided in two groups, whether the *N*-acyl chain is longer or shorter than 10 carbon atoms. From these observations, a model for the NAPE bilayer organization has been proposed: when the *N*-acyl chain contains 10 carbon atoms or more, it is anchored into the bilayer, while the chain remains at the interface for shorter *N*-acyl chain derivatives.

In the present work, Fourier transform infrared spectroscopy (FTIR) has been used to characterize the thermotropic behavior and the molecular orientation of DPPE and of two of its NAPE derivatives, with deuterated *N*-acyl chains of 6 and 16 carbon atoms, *N*-C6d- and *N*-C16d-DPPE, respectively. It was thus possible to follow independently the conformational order and the molecular orientation of the proteated acyl chains attached to the glycerol moiety of PE from the 2800–3000-cm^{-1} region, while the behavior of the deuterated *N*-acyl chain of the headgroup was monitored using the CD_2 stretching vibrations, in the 2050–2250-cm^{-1} range. Spectra were obtained, as a function of temperature, by transmission measurements for aqueous dispersions of the lipids and by polarized attenuated total reflection (ATR) for both dry and hydrated films.

MATERIALS AND METHODS

Sample preparation

Dipalmitoylphosphatidylethanolamine was purchased from Sigma (St. Louis, MO) and from Avanti Polar Lipids (Alabaster, AL), while deuterated hexadecanoic and hexanoic acids were obtained from CDN Isotopes (Canada). Deuterated *N*-acyl-DPPE were synthesized as described by Akoka et al. (1988). The products were purified by high performance liquid chromatography on a 250 × 10 mm silica column (Phenomenex Spherex 10) eluted by a $CHCl_3$/MeOH/NH_4OH (80:20:2) mixture, with a flow rate of 2 ml/min. Synthesis was monitored from the appearance of the amide bands in the infrared spectra and the purification was controlled by thin layer chromatography on silica plates.

Aqueous lipid dispersions (5–10% w/w) were prepared in water or D_2O, and the pH was adjusted to 7.0 using diluted HCl and NaOH solutions or DCl and NaOD solutions, respectively. The dispersions were vortexed, heated above the gel to liquid crystalline transition temperature, vortexed again, and cooled down in iced water. This treatment was repeated at least three times to ensure a good dispersion and hydration of the lipids.

Received for publication 3 July 1996 and in final form 28 February 1997.
Address reprint requests to Dr. Michel Pezolet, Dept. of Chemistry, Laval University, Quebec, Quebec G1K 7P4, Canada. Tel.: 418-656-2481; Fax: 418-656-7916; E-mail: michel.pezolet@chm.ulaval.ca.

0006-3495/97/06/2559/10 $2.00

Spectroscopic measurements

Transmission and attenuated total reflectance (ATR) infrared spectroscopy measurements were recorded with a Bomem DA3–02 and a Nicolet Magna 550 FTIR spectrophotometer, respectively, both equipped with mercury-cadmium-telluride (MCT) detectors and germanium coated KBr beamsplitters. For transmission measurements, a total of 1000 scans taken with a maximal optical retardation of 0.5 cm were coadded, triangularly apodized, and Fourier transformed to yield a resolution of 2 cm^{-1}. Lipid dispersions were inserted between two CaF_2 windows separated by a 12 μm mylar spacer and the infrared cell was placed in a thermoelectrically regulated sample holder.

For the ATR spectra, 250 scans were typically recorded, apodized using a Happ-Genzel function, and Fourier transformed to obtain a 2-cm^{-1} resolution. For these measurements, 20 μl of the aqueous dispersion was placed on a germanium parallelogram crystal (50 × 20 × 2 mm) with 45° faces, and was then spread back and forth using a Teflon bar until dry, in order to minimize the disorder of the different phospholipid domains with respect to the crystal surface (Tristram-Nagle et al., 1993). The ATR crystal was placed in a brass and Teflon thermostated cell where a cavity in the Teflon face opposing the sample allowed the injection of water or D_2O for measurements of the spectra of hydrated films. Polarized ATR spectra were first recorded for the dried films at 20°C, the complete evaporation of the solvent being verified by the absence of the intense O–H or O–D stretching bands. Then, water or D_2O was injected in the ATR cell and the temperature was raised above the gel to liquid crystalline transition temperature, and cooled down to 20°C. This heating-cooling cycle was repeated at least twice, the spectra being recorded at each step. Calculation of the dichroic ratio for the bands due to the methylene stretching modes has shown that the absolute value of the order parameter increases upon hydration of the lipid, reaching a constant level after cycling two or three times from 20°C to temperatures higher than the gel to liquid crystalline transition.

All spectral manipulations were performed using the SpectraCalc software (Galactic Industries Corp., Salem, NH).

Molecular orientation calculations

Attenuated total reflectance measurements were used to determine the average orientation with respect to the normal to the ATR crystal surface of the transition dipole moment for different molecular vibrations. The order parameter, $\langle P_2 \rangle$, can be obtained from the dichroic ratio, R_{ATR}, of the absorbances measured with the radiation polarized parallel ($A_\parallel$, p polarization) and perpendicular ($A_\perp$, s polarization) with respect to the plane of incidence of the infrared beam, $R_{ATR} = A_\parallel/A_\perp$. The values of the amplitude of the electric field of the infrared radiation in the three directions (the plane of incidence of the infrared beam is xz and the normal to the crystal surface is the z-axis) were calculated using the equations for thick films (Harrick, 1967) for a germanium crystal with a 45° angle of incidence, and considering refractive indexes of 4.00 for the Ge crystal and 1.44 for the phospholipid samples (Fringeli and Günthard, 1981). Then, the order parameter $\langle P_2 \rangle$, which is the average value of the second-order Legendre polynomial, is defined by the equation:

$$\langle P_2 \rangle = (3\langle \cos^2 \theta \rangle - 1) = \frac{R_{ATR} - 2.00}{R_{ATR} + 1.45} \qquad (1)$$

The brackets indicate that the expression is averaged over all the orientations in the sample. For an infrared vibration with a transition dipole moment oriented perfectly parallel and perfectly perpendicular with respect to the normal to the ATR crystal surface, the order parameter is equal to 1.0 and −0.5, respectively, while $\langle P_2 \rangle = 0$ for isotropic samples.

The order parameter obtained by ATR spectroscopy contains several contributions, which can each be characterized by an independent $\langle P_2 \rangle$ coefficient. Using the Legendre addition theorem, the global $\langle P_2 \rangle$ coefficient measured by ATR can be written as:

$$\langle P_2 \rangle = \langle P_2 \rangle_{ms} \langle P_2 \rangle_{sg} P_2(\cos^2 \beta) \qquad (2)$$

The $\langle P_2 \rangle_{ms}$ coefficient is associated with the mosaic spread, which is the disorder of the different phospholipid domains with respect to the surface of the crystal, while the $\langle P_2 \rangle_{sg}$ value characterizes the orientation with respect to the bilayer normal of the structural groups that give rise to the studied vibration. The $P_2(\cos^2 \beta)$ term takes into account the angle β between the transition dipole moment of the studied infrared vibration and the structural group. Since the β angle is fixed with respect to the molecular coordinates, this last term of the right-hand side of Eq. 2 is not an average and is equal to $(3 \cos^2 \beta - 1)/2$. The interpretation of the measured order parameter in relation to the different terms of Eq. 2 has recently been discussed thoroughly by Lafrance et al (1995).

RESULTS

Thermotropic behavior of deuterated NAPE

The strong bands due to the methylene symmetric (ν_s) and antisymmetric (ν_{as}) stretching vibrations, at 2850 and 2920 cm^{-1}, respectively, are spectral features that are frequently used to study the thermotropic behavior of phospholipids. In the case of deuterated chains, these bands are shifted to 2090 and 2195 cm^{-1}, respectively. Since the *N*-acyl chains of the NAPEs used in this work are deuterated, it is thus possible to study independently the orientation and conformation of the proteated acyl chains attached to the glycerol moiety of the phospholipid molecules and those of the chain attached to the amide group of the polar head.

Fig. 1 shows the C–H and C–D stretching mode regions for *N*-C6d-DPPE (*A*) and *N*-C16d-DPPE (*B*) aqueous dispersions, in both the gel and liquid crystalline phases. It is observed that nearly identical spectra are obtained for the C–H stretching mode region for the two NAPE dispersions. During the transition from the gel phase (*solid curves*) to the liquid crystalline phase (*dashed curves*), the methylene ν_s

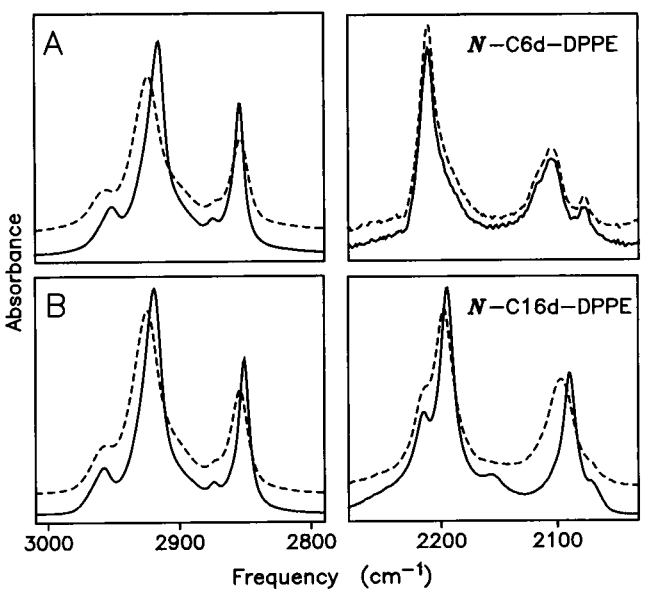

FIGURE 1 Infrared spectra showing the C–H (*left*) and C–D (*right*) stretching mode regions for (*A*) *N*-C6d- and (*B*) *N*-C16d-DPPE aqueous dispersions in the gel (*solid lines*) and liquid crystalline (*dashed lines*) phases.

and ν_{as} bands broaden and shift to higher frequencies. The frequency shift is generally associated with the introduction of *gauche* conformers in the aliphatic chains, while the band broadening can be related to a broader conformational disorder distribution or to a higher rotational mobility of the chains (Asher and Levin, 1977; Casal and Mantsch, 1983; Mantsch and McElhaney, 1991).

In contrast, the spectra obtained in the 2040–2260-cm^{-1} region for the C–D stretching vibrations of the deuterated *N*-acyl chain show striking differences between the two NAPEs. For *N*-C16d-DPPE, the shape of the spectra in this region resembles that observed in the C–H stretching mode region, showing a frequency shift and a broadening of the strong CD_2 stretching bands upon heating above the gel to liquid crystalline phase transition temperature (T_m). Due to the shorter *N*-acyl chain, the spectra recorded in this region for *N*-C6d-DPPE are dominated by the bands due to the CD_3 stretching vibrations, the CD_2 stretching bands appearing only as shoulders. A similar spectrum has also been observed for deuterated caproic acid (not shown). It can also be seen in Fig. 1 *A* that, for *N*-C6d-DPPE, the shape of the spectra recorded in the C–D stretching mode region is almost identical in the gel and in the liquid crystalline phases, and thus does not show any evidence of a phase transition.

Fig. 2 presents spectra measured in the region of the ester carbonyl stretching vibration and amide I vibration, between 1780 and 1580 cm^{-1}, for *N*-C6d- and *N*-C16d-DPPE at 20°C in the dry state and at similar reduced temperatures in the gel (T_m − 23°C) and liquid crystalline (T_m + 17°C) phases for hydrated multilayers. The asymmetric peak due to the ester carbonyl stretching vibration, which is centered near 1740 cm^{-1}, can be resolved in at least two components. The high- and low-frequency components can be assigned to non-hydrogen bonded and hydrogen bonded ester carbonyl groups, respectively (Lewis et al., 1994; Blume et al., 1988). For the different samples studied in this work, these two resolvable components arise near 1740 ± 2 and 1726 ± 3 cm^{-1}, in good agreement with previous results (Lewis et al., 1994). For the two *N*-acyl DPPE derivatives, the addition of water (or D_2O) in the ATR cell and, thereafter, the heating through the transition from the gel phase to the liquid crystalline phase cause successive increases of the intensity of the low-frequency component, I_L, at the expense of the intensity of the high-frequency one, I_H.

Fig. 2 also shows the amide I band of the *N*-acyl chain amide groups in the 1680–1600 cm^{-1} region. For *N*-C6d-DPPE in the dry state, the amide I band is located at 1642 cm^{-1}, while it is centered near 1625 and 1635 cm^{-1} for the hydrated samples in the gel and in the liquid crystalline phases, respectively. Fourier self-deconvolution of this composite band have shown that the shift to lower frequencies in the hydrated samples results from the increase of a strong component of the amide I band near 1623 cm^{-1} and of a weaker one near 1609 cm^{-1} (not shown). The 1623-cm^{-1} component can probably be assigned to amide groups involved in hydrogen bonding with water molecules, while the assignment of the lower frequency component remains

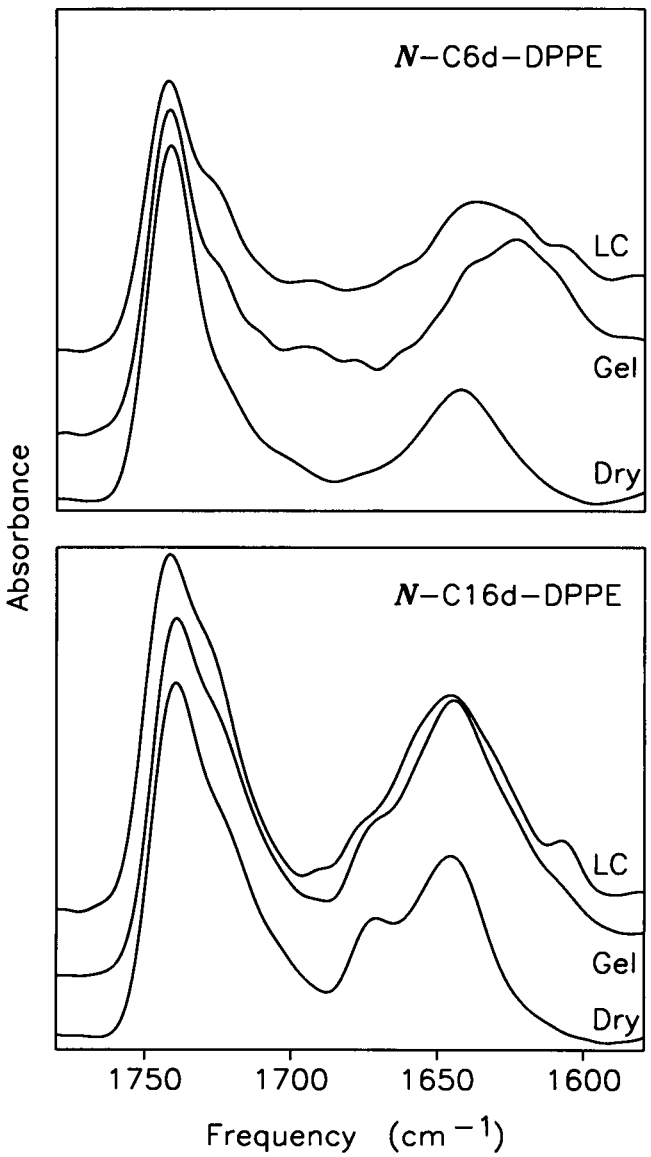

FIGURE 2 Infrared spectra showing the carbonyl stretching and the amide I vibrations for *N*-C6d-DPPE and *N*-C16d-DPPE in dry films (20°C) and in hydrated films in the gel (T_m − 23°C) and liquid crystalline (LC) (T_m + 17°C) phases.

unclear. For *N*-C16d-DPPE in the dry films, the amide I band shows two maxima located near 1670 and 1643 cm^{-1}. In the hydrated samples, the former component is not well resolved and is displayed as a shoulder on the high-frequency side of the main component of the band, which is broadened but remains centered at 1643 cm^{-1}. As observed for *N*-C6d-DPPE, a shoulder can also be distinguished near 1608 cm^{-1} in the spectra recorded for samples in the liquid crystalline phase. To investigate the nature of the 1670-cm^{-1} component of the amide I band for *N*-C16d-DPPE, spectra were recorded for mixtures of this lipid with DPPC at 1:1 and 1:3 ratios, i.e., 50% and 25% NAPE, respectively. These spectra, which are presented in Fig. 3, show that as the fraction of the long *N*-acyl chain NAPE in the mixture

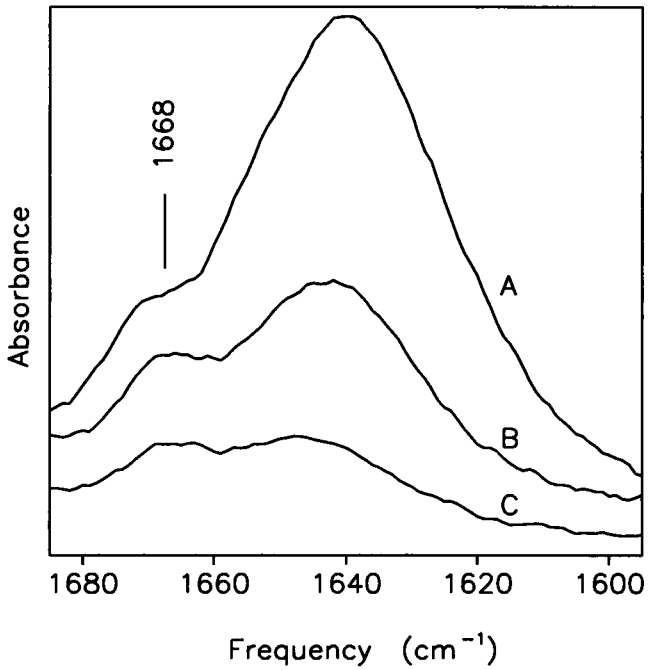

FIGURE 3 Infrared spectra in the amide I region for (*A*) pure *N*-C16-DPPE and of mixtures for *N*-C16-DPPE with DPPC at (*B*) 1:1 and (*C*) 1:3 molar ratios.

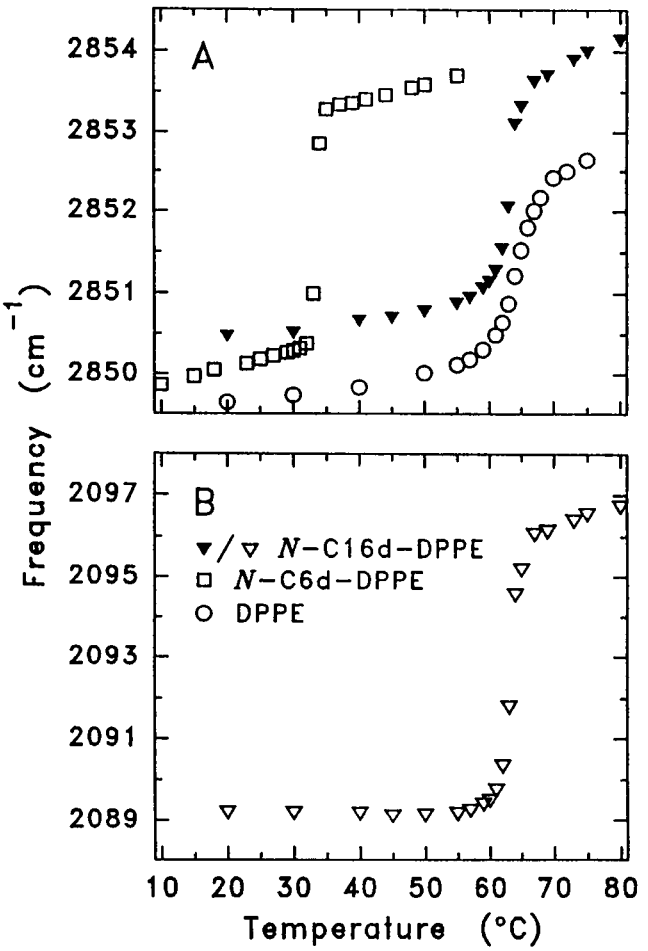

FIGURE 4 Temperature dependence of the frequency of (*A*) the CH_2 symmetric stretching vibration for DPPE, *N*-C6d-DPPE, and *N*-C16d-DPPE aqueous dispersions and (*B*) the CD_2 symmetric stretching vibration for *N*-C16d-DPPE.

decreases, the area under the 1670-cm^{-1} component increases with respect to that of the whole amide I band.

The thermotropic behavior of *N*-C6d- and *N*-C16d-DPPE aqueous dispersions is compared to that obtained for DPPE in Fig. 4 *A*, which presents the evolution of the frequency of the methylene symmetric stretching band as a function of temperature. Similar results were obtained for the ν_{as} stretching modes (not shown). The curves measured for the three samples show a well-defined highly cooperative transition. The gel-to-liquid crystalline transition temperature of 63°C observed for *N*-C16d-DPPE is close to that of DPPE, 64°C, while T_m = 33°C for the short-chain *N*-acyl derivative. These values agree well with those previously reported for non-deuterated NAPEs (Newman et al., 1986; Lafrance et al., 1990; Domingo et al., 1995). Fig. 4 *A* shows that, at equally reduced temperatures, comparable frequencies are measured for the symmetric methylene stretching mode band of DPPE and of *N*-C6d-DPPE in the gel phase, while for *N*-C16d-DPPE the ν_s vibration is centered near 2850.5 cm^{-1}, ~0.9 cm^{-1} higher than the frequency measured for DPPE.

Fig. 4 *B* presents the evolution as a function of temperature of the frequency of the CD_2 symmetric stretching band of *N*-C16d-DPPE. As observed for the CH_2 stretching vibration (Fig. 4 *A*), a sharp transition occurs at 63°C. For the *N*-C6d-DPPE, it was not possible to determine the frequency of the CD_2 symmetric or antisymmetric stretching bands without considerable uncertainty, although tentative resolution enhancement by Fourier self-deconvolution have shown that the frequency of these bands is constant within the studied temperature range. The frequency of the CD_2 ν_s band remains located near 2100 cm^{-1} from 15°C to 50°C, a value that is characteristic of a highly disordered chain (compare to the frequencies in Fig. 4 *B*). Moreover, the lack of transition for *N*-C6d-DPPE was verified by the absence of bands in the difference spectrum obtained by subtracting a spectrum measured in the gel phase (T_m − 23°C) from that measured in the liquid crystalline phase (T_m + 17°C) (curves not shown).

Orientation of the acyl chains

Table 1 presents values of the order parameter obtained by ATR measurements for the C–H and C–D stretching vibration bands for dried lipid films at 20°C, and for the hydrated films in the gel phase at a similar reduced temperature (T_m − 23°C). These average $\langle P_2 \rangle$ coefficients were found to be reproducible to ±0.01 between different samples. It is observed that, for the CH_2 stretching modes, the $\langle P_2 \rangle$ coefficients calculated from the ν_{as} band are always slightly smaller, in absolute value, than those calculated from the ν_s

TABLE 1 Order parameters calculated for the transition dipole moments of the CH_2 and CD_2 stretching vibrations of lipid films

		$\langle P_2 \rangle$					
		DPPE		*N*-C6d-DPPE		*N*-C16d-DPPE	
Vibration	Frequency (cm^{-1})	Dry	Gel	Dry	Gel	Dry	Gel
ν_{as} CH_2	2920	−0.37	−0.39	−0.40	−0.40	−0.35	−0.38
ν_s CH_2	2850	−0.39	−0.42	−0.42	−0.40	−0.36	−0.39
ν_{as} CD_2	2195	—	—	−0.03*	—#	−0.34	−0.40
ν_s CD_2	2090	—	—	−0.02*	—#	−0.34	−0.40

Films were supported on a Ge ATR crystal in the dry state, at 20°C, and after hydration with D_2O, in the gel phase at T_m −23°C.
*Calculated using Fourier self-deconvolution and curve fitting procedures (±0.05).
#These bands are too weak to give reproducible results.

band. This is explained by the fact that two broad Fermi resonance bands contribute to the spectra in the region of the 2920-cm^{-1} vibration, while the 2850-cm^{-1} feature is better resolved from other bands (Snyder et al., 1978). The $\langle P_2 \rangle$ values obtained from the CH_2 ν_s band can thus be considered as more representative of the *true* orientation of the acyl chains.

For the dry films of the three lipids studied in this work, the order parameter measured for the CH_2 stretching bands are approximately equal to −0.4, which indicates a quite high orientation of the plane of the methylene groups perpendicular to the reference direction (i.e., the normal to the ATR crystal surface). For DPPE and *N*-C16d-DPPE, the order parameter becomes more negative upon addition of water, which suggests an increase of the order in the hydrated samples as compared to the dry films.

The $\langle P_2 \rangle$ coefficient characterizing the orientation of the transition moment of the CD_2 stretching vibrations of *N*-C6d-DPPE samples in the dry state is close to zero. It was not possible to calculate the order parameter value from the spectra of hydrated *N*-C6d-DPPE samples, because the weak bands arising from the C–D stretching mode region are superimposed over either the H_2O association band centered near 2125 cm^{-1}, or the tail of the strong D_2O stretching absorption band located near 2500 cm^{-1}. The calculation of the dichroic ratio after subtraction of the water spectra, or using polynomial baselines, led to irreproducible results.

Table 1 shows that, for *N*-C16d-DPPE in the dry films and in the hydrated samples in the gel phase, the orientation of the proteated acyl chains is similar to that of the deuterated *N*-acyl chain. Fig. 5 demonstrates that this excellent correlation of the order parameters calculated for the CH_2 and CD_2 symmetric stretching vibrations is observed over the full temperature range that has been studied for this lipid. A comparison of the shape of the curves presented in Figs. 4 and 5 suggests that a close relationship could exist between the temperature dependence of the frequency shift and of the order parameter. Actually, it is shown in Fig. 6 *A* that a plot of the frequency of the CH_2 and CD_2 stretching bands as a function of their respective $\langle P_2 \rangle$ coefficient gives a linear correlation for *N*-C16d-DPPE for both vibrations. Furthermore, Fig. 6 *B* shows that such a linear relationship is also observed between the $\langle P_2 \rangle$ coefficient and the frequency measured for the CH_2 stretching vibrations of DPPE and *N*-C6d-DPPE, the results from the three different samples being superimposed on a common line. For *N*-C6d-DPPE, there are small deviations from the common curve at high (gel phase) and low (LC phase) $\langle P_2 \rangle$ values.

Orientation of the carbonyl groups

Table 2 presents the results of deconvolution and curve-fitting calculations that were conducted to evaluate the orientation of the high- and low-frequency components of the carbonyl stretching band. These are average results of, at least, five curve fitting calculations conducted on the polarized infrared spectra measured for two different samples of each lipid. A linear baseline was subtracted from the spectra before the fitting procedure. The fit was then obtained using two components under the $\nu_{C=O}$ band and, for the NAPE spectra, two other components were used under the amide I band. For the three phospholipids, the low-frequency component of the ester carbonyl stretching band is broader than the higher-frequency one, which can be explained by a

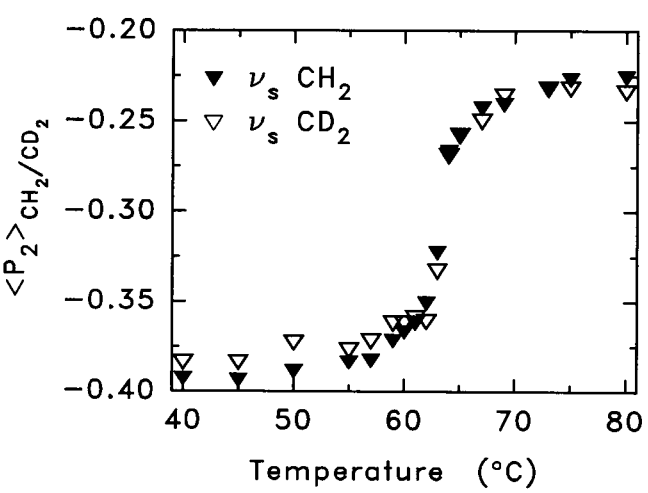

FIGURE 5 Effect of temperature on the order parameter $\langle P_2 \rangle$ calculated from the dichroic ratio measured by ATR for the CH_2 and CD_2 symmetric stretching vibrations for *N*-C16d-DPPE.

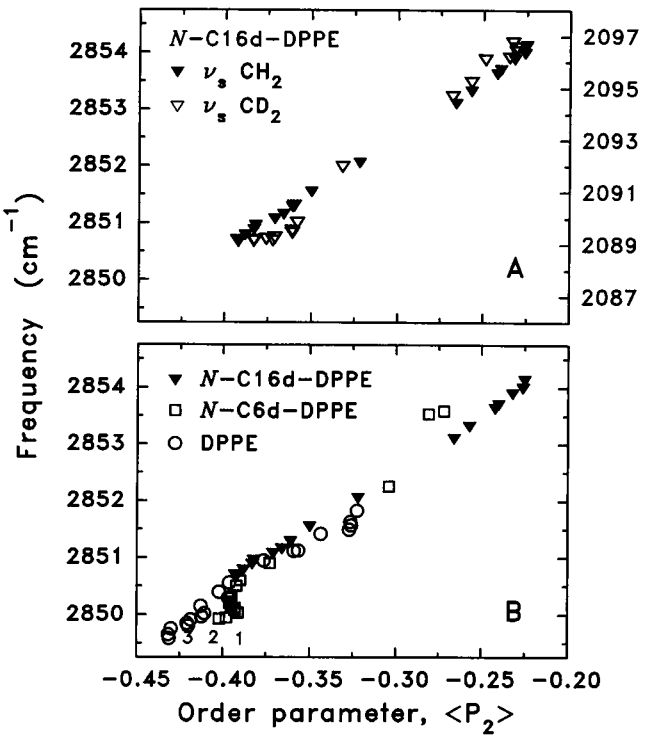

FIGURE 6 Variation of the frequency of the methylene symmetric stretching vibration as a function of the order parameter. (*A*) ν_s CH_2 and ν_s CD_2 bands for *N*-C16d-DPPE, and (*B*) ν_s CH_2 band for DPPE, *N*-C6d-DPPE, and *N*-C16d-DPPE.

broad distribution of the hydrogen bond strengths. Consequently, the position of the high-frequency component could be determined with a better accuracy than that of the lower-frequency component. The curve-fitting results presented in Table 2, obtained on the raw spectra of the lipids, were compared to results calculated with Fourier self-deconvoluted spectra, and a good correlation was found between the two sets. Fig. 7 shows a typical fit, with the shape of the two components of the $\nu_{C=O}$ band, for *N*-C16d-DPPE in dry and hydrated samples in the gel phase.

For DPPE, as well as for the deuterated NAPE samples in the gel phase, the $\langle P_2 \rangle$ coefficients obtained for the two components of the carbonyl stretching band are comparable, within the experimental error. On the other hand, for the NAPEs in the dried films, order parameter values ~ -0.3 are calculated for the high-frequency component, while the low-frequency component gives a smaller value of $\langle P_2 \rangle = -0.15$. These results indicate that the carbonyl groups giving rise to the low-frequency component in the dry films, which can be C=O groups involved in intra or intermolecular hydrogen bonds, either possess a broad orientation distribution or are oriented, in the average, at an angle closer to the so-called "magic angle" of 54.7°, where $(3 \cos^2 \theta - 1)/2 = 0$ (Lafrance et al., 1995). Moreover, the ratio of the integrated intensities under the high- and low-frequency components of the carbonyl stretching band indicate that there is a higher proportion of hydrogen-bonded carbonyl groups in NAPEs as compared to DPPE.

For the amide I band of *N*-C16d-DPPE, an identical order parameter of -0.32 is obtained for both the dry films and the hydrated samples in the gel phase. In contrast, the frequency shift observed upon hydration of the short *N*-acyl chain derivative (Fig. 2) is accompanied by a reorientation of the amide groups, the $\langle P_2 \rangle$ value of the amide I band varying from -0.26 to -0.33. Curve-fitting calculations failed to give conclusive information on the behavior of the different components of this band, mostly because of the overlap with the amide II band, which render it difficult to obtain a reproducible shape on the low-frequency side of the amide I band.

DISCUSSION

Acyl chain region

A first conclusion that emerges from this study on NAPE phospholipids bearing deuterated *N*-acyl chains is evidenced by the parallel behavior of the proteated and deuterated acyl chains of *N*-C16d-DPPE. As observed in Fig. 4, the transition temperature for the gel-to-liquid crystalline phase transition occurs at 63°C for both the headgroup chain and for those attached to the glycerol moiety of the phospholipid. Furthermore, Fig. 5 shows that a sharp decrease of the $\langle P_2 \rangle$ coefficient calculated for these same bands occurs at the same temperature. This variation can be ascribed to an

TABLE 2 Order parameter values calculated for the carbonyl stretching band and for its high and low frequency components from ATR spectra of lipid films

				High-frequency component		Low-frequency component	
Sample		Overall $\langle P_2 \rangle$ (± 0.01)	I_H/I_L	ν (cm^{-1}) $\pm$ 0.3	$\langle P_2 \rangle \pm 0.02$	ν (cm^{-1}) $\pm$ 0.8	$\langle P_2 \rangle \pm 0.02$
DPPE	Dry	−0.28	1.80	1738.8	−0.29	1723.5	−0.25
	Gel	−0.32	0.93	1741.3	−0.33	1724.3	−0.32
N-C6d-DPPE	Dry	−0.23	1.02	1741.7	−0.29	1725.1	−0.14
	Gel	−0.34	0.45	1741.9	−0.35	1724.5	−0.34
N-C16d-DPPE	Dry	−0.21	0.45	1741.2	−0.32	1726.0	−0.15
	Gel	−0.34	0.30	1741.1	−0.37	1727.8	−0.33

Values calculated in the dry state, at 20°C, and in the gel phase after hydration in D_2O ($T_m - 23°C < T < T_m - 13°C$), and ratio I_H/I_L of the integrated intensities of the high frequency component over the low frequency component.

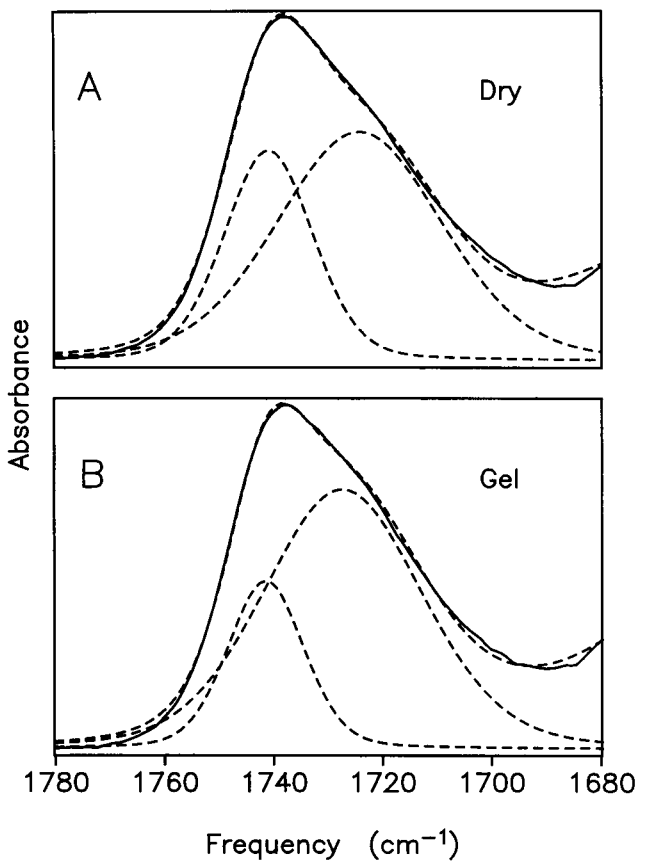

FIGURE 7 Typical results of curve-fitting calculations for the ester carbonyl stretching band (*A*) dry films and (*B*) hydrated samples in the gel phase of *N*-C16d-DPPE. Full curves: original spectra; dotted curves: high- and low-frequency components of the band and resulting fit.

increase of the conformational disorder caused by the introduction of *gauche* conformers in both the proteated and deuterated acyl chains during the transition. Fig. 5 also reveals that the molecular orientation of the three acyl chains of *N*-C16d-DPPE remains almost identical over the full temperature range that has been investigated. These results demonstrate unambiguously the deep penetration of the *N*-C16 chain into the hydrophobic region of the lipid bilayer, as it was suggested in previous studies of NAPEs by NMR, Raman, and infrared spectroscopies (Akoka et al., 1988; Lafrance et al., 1990).

The slightly higher frequency observed in Fig. 4 A for the symmetric methylene stretching mode band of *N*-C16d-DPPE in the gel phase, as compared to DPPE, could indicate a higher level of conformational disorder in the long *N*-acyl chain derivative. However, this frequency is also slightly higher than that previously reported for undeuterated *N*-C16-DPPE (Lafrance et al., 1990). The high frequency of the 2850-cm^{-1} band is most likely due to the isotopic dilution effect, since shifts toward higher frequencies have been observed for the methylene stretching modes when proteated hydrocarbon chains are diluted in their perdeuterated analogs (Kodati et al., 1994; Nabet et al., 1996). The isotropic dilution effect results from a decrease of interchain vibrational coupling caused by the incorporation of the deuterated chains with the bilayer (Kodati et al., 1994). It is not possible to determine whether the higher frequency measured for *N*-C16d-DPPE in the gel phase results from isotopic dilution or from a higher conformational disorder.

For *N*-C6d-DPPE, the shape of the bands due to the CD stretching vibrations (Fig. 1), and the high frequency, ~2100 cm^{-1}, observed for the CD_2 ν_s mode in the deconvolved spectra of the lipid in both the gel and LC phases, indicate that the headgroup chain is disordered and do not display any evidence of phase transition. In the dry films, the order parameter calculated for the transition moments of the CD_2 stretching vibrations is close to zero (Table 1), suggesting that the short deuterated chain is random. At equal reduced temperatures, comparable frequencies are measured for the CH_2 ν_s vibration of DPPE and of *N*-C6d-DPPE in the gel phase (Fig. 4 *A*), which indicates that the conformational order in the hydrophobic region of the bilayer is not perturbed by the six-carbon *N*-acyl chain. These observations demonstrate that the short *N*-C6 chain is not anchored deeply into the hydrophobic region of the membranes, as suggested by Akoka et al. (1988) and Lafrance et al. (1990).

The exact location of the short *N*-acyl chain in *N*-C6d-DPPE bilayers remains unclear. The inclusion of a few methylene groups of the headgroup chain can be expected to have a disrupting effect on the conformational order of the upper part of the acyl chains, near the glycerol moiety. Since the frequency and the order parameter measured in the CH_2 stretching vibrations for *N*-C6d-DPPE in the gel phase are comparable to those obtained for DPPE and *N*-C16d-DPPE, as evidenced in Fig. 4 and Table 1, it seems most probable that the six-carbon chain is located somewhere in the polar region.

A somewhat surprising observation made in the present study is the linear relationship between the temperature-induced frequency shift of the CH_2 and CD_2 stretching bands and the order parameter (Fig. 6). This type of behavior has previously been reported between the frequency of the CH_2 stretching vibrations and the order parameter measured by NMR spectroscopy (Kodati and Lafleur, 1993), but in the liquid crystalline phase only. The results obtained in the present work demonstrate that the linear correlation between the $\langle P_2 \rangle$ coefficient and the frequency of the CH_2 and CD_2 ν_s or ν_{as} stretching bands prevails for different lipid systems, in the gel phase and during the phase transition as well as in the LC phase.

The $\langle P_2 \rangle$ coefficient measured for phospholipid samples deposited on solid supports depends on the mosaic spread, on the variation of the chain tilt angle with respect to the bilayer normal, and on the conformational order. Furthermore, Kodati et al. (1994) have pointed out that, apart from conformational disorder, the frequency shift of the methylene stretching vibrations can also be related to intermolecular chain coupling and librotorsional motions of the carbon backbone. The linear correlations observed in Fig. 6 indi-

cate that, in the orientation measurements reported herein, it is most probable that the conformational disorder along the acyl chains governs the variation of both the order parameter and of the frequency shift of the CH_2 and CD_2 ν_s and ν_{as} bands. Actually, it is unlikely that variations of different factors at the molecular level influence two measurable parameters in such a way that a linear relationship is obtained. Thus, the fact that the results obtained for the CH_2 stretching bands for the two NAPEs and for DPPE fit on the same line, as shown in Fig. 6 *B*, demonstrates that the acyl chains of the three lipids most probably have orientation distributions of comparable shapes and are oriented at the same tilt angle with respect to the normal to the bilayer surface.

The linear correlation between the order parameter, measured either by NMR or infrared spectroscopy, and the frequency of the CH_2 or of the CD_2 stretching vibrations has, until now, been observed for various phospholipids, with different acyl chain lengths, degree of insaturation, and headgroups (NAPEs, DPPE, DMPE, POPE, POPC, DPPC, and DMPC), as well as for phosphatidylcholines in the presence of cholesterol (POPC, DMPC, and DPPC) (Kodati and Lafleur, 1993; Pézolet, Lafrance, and Le Bihan, unpublished results; this work). To our knowledge, there is no report in the literature discussing the relationship between the order parameters measured by NMR and by infrared spectroscopy. While these two techniques determine the molecular orientation at different time scales, both are used to calculate the average coefficient of the second-order Legendre polynomial, $(3\cos^2\theta - 1)/2$, for the orientation of the CH_2 or CD_2 groups. The order parameter obtained by NMR spectroscopy averages the "wobbling in the cone" of the molecular chain, and thus determines the average solid angle encompassing the movement of the chain measured in the NMR time domain. The order parameter obtained by IR spectroscopy, measured over a much shorter time, corresponds to a molecular "snapshot" that averages the orientation of chains in fixed conformations. The linear relationships obtained between the frequency shift of infrared bands and the order parameter determined by NMR (Kodati and Lafleur, 1993) and by infrared spectroscopy (this work) seem to indicate that both methods give similar information, and that averaging over the movement of the chains is equivalent to averaging over a great number of chains in different, but fixed, conformations.

It can be suggested that plots of the frequency of the CH_2 ν_s or ν_{as} bands as a function of the $\langle P_2\rangle$ coefficient can be used to determine the effect of different parameters on the behavior of phospholipids. For example, a horizontal translation of the linear plots of Fig. 6 could be interpreted by a variation of the mosaic spread. Such translations were indeed observed between the orientation measurements made at 20°C on the dry films of DPPE and NAPEs and those made at the same temperature after addition of water in the ATR cell. This is shown by the numbered points in Fig. 6 *B* that correspond to the average coordinates measured for three DPPE films (1, in the dry state; 2, after 5–10 min in D_2O; 3, after the first heating cycle over T_m). For these samples, a constant value of the $\langle P_2\rangle$ coefficient was reached after the second heating-cooling cycle). This horizontal translation, which occurred with a negligible ± 0.04 cm^{-1} variation in the frequency of the CH_2 stretching bands, can be explained by a reorientation of the bilayer domains on the ATR crystal surface (i.e., a decrease of the mosaic spread), induced by the fluidity of the hydrated system.

The results presented in Table 1 indicate that the order parameter measured for the proteated acyl chains of *N*-C16d-DPPE is slightly smaller than that obtained for DPPE or for *N*-C6d-DPPE, in the dry films as well as in the gel phase of hydrated samples. Assuming that the coincidence on a single line of the results presented in Fig. 6 *B* indicates that the mosaic spread is comparable in all studied samples, the smaller $\langle P_2\rangle$ coefficients obtained for *N*-C16d-DPPE can be ascribed to a slightly higher conformational disorder of the acyl chains linked to the glycerol moiety. This disorder can result from the introduction of *gauche* conformers to accommodate the *N*-acyl chain in the bilayer.

The results presented in Figs. 5 and 6 demonstrate the usefulness of the measurement of the variation of the order parameter in thermotropic studies of lipids. However, it is also of interest to consider the absolute significance of the $\langle P_2\rangle$ values. Assuming that the acyl chains are in an all-*trans* conformation in the gel phase, the order parameter can be used to calculate the tilt angle of the chains with respect to the normal to the bilayer surface, θ_{tilt} (Fringeli, 1977; Fringeli and Günthard, 1981; Goormaghtigh and Ruysschaert, 1990). The crystal structure of dilauryl-PE (DLPE) shows that its acyl chains are perpendicular to the bilayer plane ($\theta_{tilt} = 0°$, Hitchcock et al., 1974), and it has been shown that this orientation is retained in dried and hydrated films of DPPE (McIntosh, 1980). Then, taking values of $P_2(\cos^2\beta) = -0.5$ and $\langle P_2\rangle_{ms} = 1$ in Eq. 2, and a narrow orientation distribution of the acyl chains along the normal to the bilayer plane (Lafrance et al., 1995), a $\langle P_2\rangle$ coefficient of -0.5 should be obtained for the CH_2 stretching modes. However, the order parameter of -0.42 measured for the CH_2 ν_s vibration for DPPE (Table 1) rather corresponds to a $\theta_{tilt} \approx 19°$, using the above values for $P_2(\cos^2\beta)$ and $\langle P_2\rangle_{ms}$ in Eqs. 1 and 2. This result agrees well with previous FTIR spectroscopy studies, which reported θ_{tilt} angle values between 10° and 25° for DPPE (Akutsu et al., 1975; Fringeli, 1977).

The discrepancy between the measured $\langle P_2\rangle$ coefficient and that corresponding to a perfect perpendicular orientation of the chains with respect to the bilayer plane can be explained by a combination of three factors: 1) the bending of the *sn*-2 chain near the glycerol moiety (Hitchcock et al., 1974); 2) the presence of a 2–7% fraction of methylene groups involved in *gauche* bonds in the gel phase (see Lafrance et al., 1995); and 3) values of $\langle P_2\rangle_{ms} \sim 0.9$ for the mosaic spread of supported lipid samples (Rothschild and Clark, 1979; Clark et al., 1980). Taken alone, none of these factors can account for the low values of the order parameter calculated for DPPE. However, simulations demonstrate that the $\langle P_2\rangle$ value is most strongly affected by the mosaic spread or by the conformational disorder for orien-

tation distributions centered around the normal to the crystal surface, i.e., $\theta_{tilt} = 0°$ (Lafrance et al., 1995). Therefore, moderate estimates of the mosaic spread and of the fraction of *gauche* conformers ($\langle P_2 \rangle_{ms} = 0.9$, 6% of methylene groups involved in *gauche* bonds) can explain the $\langle P_2 \rangle$ values calculated for DPPE. Assuming that the superimposition of these two types of disorder can be described by a smooth distribution resulting from a 50% Gaussian + 50% Lorentzian sum (Lafrance et al., 1995), an orientation distribution of the acyl chains centered about the normal to the ATR crystal surface with a full-width at half-height of 20° would account for the $\langle P_2 \rangle$ value of -0.42 measured for the dipole transition moment of the CH_2 symmetric stretching vibration for DPPE.

Interfacial and headgroup region

For the three lipids investigated, hydration of the samples and heating from the gel phase to the LC phase both result in a decrease of the intensity of the high-frequency component of the carbonyl stretching band at the expense of that of the low-frequency component (Fig. 2 and Table 2). The decrease of the I_H/I_L ratio upon hydration of the samples most probably results from hydrogen bonding of a fraction of C=O groups to water molecules. The further decrease of this intensity ratio during the phase transition of the lipids indicates a higher proportion of hydrogen-bonded carbonyl groups in the liquid crystalline phase compared to the gel phase, as it has generally been observed for most phospholipids (Blume et al., 1988) and also for *N*-acyl DPPEs (Lafrance et al., 1990). It can be observed in Table 2 that *N*-C16d-DPPE shows a much weaker decrease of the I_H/I_L ratio upon hydration than the two other lipids. Moreover, the addition of water to dry *N*-C16d-DPPE films causes only a minor broadening of the amide I band (Fig. 2), without any frequency shift, while this band gives an identical order parameter for dry films and hydrated samples in the gel phase. These results indicate that the headgroup region of *N*-C16d-DPPE is not easily accessible to the solvent.

The spectra presented in Fig. 3 indicate that when the concentration of *N*-C16-DPPE in a matrix of DPPC is decreased, the intensity of the 1670-cm^{-1} component increases at the expense of the intensity of the 1640-cm^{-1} component. Since the dilution of the long-chain NAPE in a matrix of DPPC decreases the probability of having adjacent NAPE molecules linked by intermolecular hydrogen bonding, the 1640-cm^{-1} component of the amide band can be assigned to amide groups where both the C=O and N–H groups are involved in intermolecular bonds, while the 1670-cm^{-1} component could be associated to amide groups where only the N–H groups are involved in such bonds, in agreement with the conclusions of de Lozé et al. (1978). This assignment is further supported by the results of Domingo et al. (1994), who have studied the behavior of NAPEs of natural origin and their *N*-methylated derivatives. While the 1670-cm^{-1} component of the amide I band is clearly displayed in the Fourier deconvolved spectra of these natural NAPEs with long chains, it is absent from that of the *N*-Me-NAPEs, which cannot undergo hydrogen bonding through the amine group. It is also known that *N*-methylation of DPPE causes a decrease of the T_m (Casal and Mantsch, 1984; Brown et al., 1986), resulting from the disruption of the tight hydrogen bond network of phosphatidylethanolamines, which links the amine hydrogen atoms to the phosphoryl groups of adjacent molecules (Hitchcock et al., 1974; Hauser et al., 1981). However, the almost identical T_m for DPPE and *N*-C16d-DPPE (Fig. 4) shows that the strength of the lipid-lipid interactions are comparable in both phospholipids. Therefore, the reduced hydrogen bonding capacity caused by the substitution of one hydrogen atom of the amine group by a long acyl chain is compensated by the formation of intermolecular hydrogen bonds involving the amide groups, in agreement with the conclusions of previous workers (Akoka et al., 1988; Lafrance et al., 1990; Domingo et al., 1994). In addition, the low I_H/I_L measured for *N*-C16d-DPPE, as compared to the other two lipids (Table 2), indicates that a significant fraction of the C=O groups are hydrogen-bonded, even in the dry samples. It can be postulated that, while the amine group of DPPE is located near the bilayer surface (Hitchcock et al., 1974; Hauser et al., 1981), the amide group of NAPEs is located closer to the interfacial region, and that some of the N–H groups can undergo hydrogen bonding with the ester carbonyl groups. This different headgroup conformation of *N*-C16d-DPPE in comparison to DPPE is possibly favored by the anchoring of the *N*-acyl chain deep in the hydrophobic region.

For *N*-C6d-DPPE, the 18-cm^{-1} decrease of the position of the amide I band upon hydration indicates that the amide groups are strongly solvated and the variation of the order parameter shows that a reorientation of these groups also occurs. The shift toward higher frequency of the amide I band observed when the samples are heated from the gel phase to the LC phase can be explained by a weakening of the hydrogen bonds with water molecules at higher temperature.

The spectra of hydrated *N*-C6d-DPPE samples do not show the presence of a component of the amide I band near 1670 cm^{-1}, indicating that the N–H groups are probably not involved in intermolecular hydrogen bonding. The low gel-to-liquid crystalline temperature of *N*-C6d-DPPE (Fig. 4), and other NAPEs with a short *N*-acyl chain in comparison to DPPE, can thus be explained by the steric hindrance caused by the presence of the *N*-acyl chain in the headgroup region, which probably precludes the formation of strong lipid-lipid interactions (Lafrance et al., 1990; Akoka et al., 1988).

CONCLUSION

The independent measurements of the molecular orientation of the glycerol proteated acyl chains and of the deuterated *N*-acyl chain of *N*-C16d-DPPE demonstrate that the latter chain is embedded deeply into the hydrophobic region of the bilayer. For *N*-C6d-DPPE, the order parameter calcu-

lated for the *N*-acyl in the dry samples, and the shape of the spectra in the C–D stretching vibration region, indicates that the short chain is disordered.

It is shown that a plot of the frequency of the methylene C–H stretching vibrations as a function of the corresponding order parameter gives a linear relationship. Since the results obtained for the three lipids investigated fall on a single line, it is concluded that the acyl chains for both NAPEs are parallel to the normal to the bilayer, as it is found for DPPE. The discrepancy between the $\langle P_2 \rangle$ values measured by infrared spectroscopy and the value indicative of a perfect orientation perpendicular to the ATR crystal surface is explained by a small fraction of *gauche* conformers and by a mosaic spread of the lipid domains on the ATR crystal.

The analysis of the shape of the ester carbonyl stretching vibration demonstrate that, in both dry and gel phase samples, the fraction of hydrogen-bonded C=O groups is higher in the NAPEs than in DPPE, particularly for *N*-C16d-DPPE. Moreover, for this latter lipid, the position of the amide I band indicates that the N–H groups are also involved in hydrogen bonds. It is thus suggested that the relatively high gel-to-liquid crystalline phase transition temperature of long *N*-acylated PEs is explained by their headgroup conformation, where intermolecular hydrogen bonds link the amide and the ester carbonyl groups. This headgroup conformation is probably favored by the insertion of the *N*-acyl chain deep in the hydrophobic region. In contrast, for short-chain NAPEs characterized by low T_m values, the presence of the short *N*-acyl chain in the headgroup region precludes the formation of such a network of intermolecular hydrogen bonds.

REFERENCES

Akoka, S., C. Tellier, C. Le Roux, and D. Marion. 1988. A phosphorus magnetic resonance spectroscopy and a differential scanning calorimetry study of the physical properties of *N*-acylphosphatidylethanolamines in aqueous dispersions. *Chem. Phys. Lipids.* 46:43–50.

Akutsu, H., Y. Kyogoku, H. Nakahara, and K. Fukuda. 1975. Conformational analysis of phosphatidylethanolamine in multilayers by infrared spectroscopy. *Chem. Phys. Lipids.* 15:222–242.

Asher, I. M., and I. W. Levin. 1977. Effects of temperature and molecular interactions on the vibrational infrared spectra of phospholipid vesicles. *Biochim. Biophys. Acta.* 468:63–72.

Blume, A., W. Hübner, and G. Messner. 1988. Fourier transform infrared spectroscopy of ^{13}C=O-labeled phospholipids: hydrogen bonding to carbonyl groups. *Biochemistry.* 27:8239–8249.

Bomstein, R. A. 1965. A new class of phosphatides isolated from soft wheat flour. *Biochem. Biophys. Res. Commun.* 21:49–54.

Brown, P. M., J. Steers, S. W. Hui, P. L. Yeagle, and J. R. Silvius. 1986. Role of the head group structure in the phase behavior of amino phospholipids. 2. Lamellar and nonlamellar phases of unsaturated phosphatidylethanolamine analogues. *Biochemistry.* 25:4259–4267.

Casal, H. L., and H. H. Mantsch. 1983. The thermotropic phase behavior of *N*-methylated dipalmitoylphosphatidylethanolamines. *Biochim. Biophys. Acta.* 735:387–396.

Casal, H. L., and H. H. Mantsch. 1984. Polymorphic phase behavior of phospholipid membranes studied by infrared spectroscopy. *Biochim. Biophys. Acta.* 779:381–401.

Chapman, K. D., and S. M. Moore, Jr. 1993. *N*-acylphosphatidylethanolamine synthesis in plants: occurrence, molecular composition and phospholipid origin. *Arch. Biochem. Biophys.* 301:21–33.

Clark, N. A., K. J. Rothschild, D. A. Luippold, and B. A. Simon. 1980. Surface-induced lamellar orientation of multilayer membrane arrays. *Biophys. J.* 31:65–96.

de Lozé, C., M.-H. Baron, and F. Fillaux. 1978. Interactions of the CONH group in solution: interpretation of the infrared and Raman spectra in relationship to secondary structures of peptides and proteins. *J. Chim. Phys.* 75:631–649.

Domingo, J. C., M. Mora, and M. A. de Madariaga. 1994. Role of the headgroup structure in the phase behavior of *N*-acylethanolamine phospholipids: hydrogen-bonding ability and headgroup size. *Chem. Phys. Lipids.* 69:229–240.

Domingo, J. C., M. Mora, and M. A. de Madariaga. 1995. The influence of *N*-acyl chain length on the phase behavior of natural and synthetic *N*-acylethanolamine phospholipids. *Chem. Phys. Lipids.* 75:15–25.

Fringeli, U. P. 1977. The structure of lipids and proteins studied by attenuated total reflection (ATR) infrared spectroscopy. II. Oriented layers of a homologous series: phosphatidyl-ethanolamine to phosphatidylcholine. *Z. Naturforsch.* 32:20–45.

Fringeli, U. P., and H. H. Günthard. 1981. *In* Membrane Spectroscopy. E. Grell, editor. Springer, New York. 270–332.

Goormaghtigh, E., and J. M. Ruysschaert. 1990. *In* Molecular Description of Biological Membranes by Computer Aided Conformational Analysis, Vol. 1. R. Brasseur, editor. CRC Press, Boca Raton. 285–329.

Harrick, N. J. 1967. Internal Reflection Spectroscopy. John Wiley & Sons, New York.

Hauser, H., I. Pascher, R. H. Pearson, and S. Sundell. 1981. Preferred conformation and molecular packing of phosphatidylethanolamine and phosphatidylcholine. *Biochim. Biophys. Acta.* 650:21–51.

Hitchcock, P. B., R. Mason, K. M. Thomas, and G. G. Shipley. 1974. Structural chemistry of 1,2 dilauryl-DL-phosphatidylethanolamine: molecular conformation and intermolecular packing of phospholipids. *Proc. Natl. Acad. Sci. USA.* 71:3036–3040.

Kodati, V. R., R. El-Jastimi, and M. Lafleur. 1994. Contribution of the intermolecular coupling and librotorsional mobility in the methylene stretching modes in the infrared spectra of acyl chains. *J. Phys. Chem.* 98:12191–12197.

Kodati, V. R., and M. Lafleur. 1993. Comparison between orientational and conformational orders in fluid lipid bilayers. *Biophys. J.* 64: 163–170.

Lafrance, D., D. Marion, and M. Pézolet. 1990. Study of the structure of *N*-acyldipalmitoylphosphatidylethanolamines in aqueous dispersion by infrared and Raman spectroscopies. *Biochemistry.* 29:4592–4599.

Lafrance, C.-P., A. Nabet, R. E. Prud'homme, and M. Pézolet. 1995. On the relationship between the order parameter $\langle P_2(\cos\theta) \rangle$ and the shape of orientation distributions. *Can. J. Chem.* 73:1497–1505.

Lewis, R. N. A. H., R. N. McElhaney, W. Pohle, and H. H. Mantsch. 1994. Components of the carbonyl stretching band in the infrared spectra of hydrated 1,2-diacylglycerolipid bilayers: a reevaluation. *Biophys. J.* 67: 2367–2375.

Mantsch, H. H., and R. N. McElhaney. 1991. Phospholipid phase transitions in model and biological membranes as studied by infrared spectroscopy. *Chem. Phys. Lipids.* 57:213–226.

McIntosh, T. J. 1980. Differences in hydrocarbon chain tilt between hydrated phosphatidylethanolamine and phosphatidylcholine bilayers: a molecular packing model. *Biophys. J.* 29:237–246.

Nabet, A., J. A. Boggs, and M. Pézolet. 1996. Study by infrared spectroscopy of the interdigitation of C26:0 cerebroside sulfate into phosphatidylcholine bilayers. *Biochemistry.* 35:6674–6683.

Newman, J. L., D. L. Stiers, W. H. Anderson, and H. H. O. Schmid. 1986. Phase behavior of synthetic *N*-acylethanolamine phospholipids. *Chem. Phys. Lipids.* 42:249–260.

Rothschild, K. J., and N. A. Clark. 1979. Polarized infrared spectroscopy of oriented purple membrane. *Biophys. J.* 25:473–487.

Snyder, R. G., S. L. Hsu, and S. Krimm. 1978. Vibrational spectra in the C–H stretching region and the structure of the polymethylene chain. *Spectrochim. Acta.* 34A:395–406.

Tristram-Nagle, S., R. Zhang, R. M. Suter, C. R. Worthington, W.-J. Sun, and J. F. Nagle. 1993. Measurement of chain tilt angle in fully hydrated bilayers of gel phase lecithins. *Biophys. J.* 64:1097–1109.